Published in final edited form as:

Circ Cardiovasc Imaging. 2019 June ; 12(6): e008975. doi:10.1161/CIRCIMAGING.118.008975.

Diagnostic Accuracy of Advanced Imaging in Cardiac Sarcoidosis: An Imaging-Histologic Correlation Study in Patients Undergoing Cardiac Transplantation

Sanjay Divakaran, MD[1,2], **Garrick C. Stewart, MD**[2], **Neal K. Lakdawala, MD**[2], **Robert F. Padera, MD, PhD**[3], **Wunan Zhou, MD**[1], **Akshay S. Desai, MD, MPH**[2], **Michael M. Givertz, MD**[2], **Mandeep R. Mehra, MD**[2], **Raymond Y. Kwong, MD, MPH**[1,2], **Sandeep S. Hedgire, MD**[4], **Brian B. Ghoshhajra, MD, MBA**[4], **Viviany R. Taqueti, MD, MPH**[1], **Hicham Skali, MD, MSc**[1,2], **Sharmila Dorbala, MD, MPH**[1], **Ron Blankstein, MD**[1,2], **Marcelo F. Di Carli, MD**[1,2]

[1]Cardiovascular Imaging Program, Departments of Medicine and Radiology, Brigham and Women's Hospital, Harvard Medical School, Boston, Massachusetts

[2]Cardiovascular Division, Department of Medicine, Brigham and Women's Hospital, Harvard Medical School, Boston, Massachusetts

[3]Department of Pathology, Brigham and Women's Hospital, Harvard Medical School, Boston, Massachusetts

[4]Division of Cardiovascular Imaging, Department of Radiology, Massachusetts General Hospital, Harvard Medical School, Boston, Massachusetts.

Abstract

Background: The diagnostic yield of cardiac sarcoidosis (CS) by endomyocardial biopsy is limited. Fluorodeoxyglucose (FDG) positron emission tomography (PET) and cardiac magnetic resonance imaging (MRI) may facilitate noninvasive diagnosis, but the accuracy of this approach is not well defined. We aimed to correlate findings from FDG PET and cardiac MRI with histologic findings from explanted hearts of patients who underwent cardiac transplantation.

Methods: We analyzed the explanted heart histology for all patients who underwent cardiac transplant at our center from April 2008 to July 2018 and had pre-transplant FDG PET (n=18) or cardiac MRI (n=31). The likelihood of CS based on FDG PET or cardiac MRI was categorized in a blinded fashion using a previously published method.

Results: Using a CS probable cutoff for FDG PET resulted in a sensitivity of 100.0% (95% CI: 54.1% to 100.0%) and a specificity of 33.3% (95% CI: 9.9% - 65.1%). Three of the nine CS probable by FDG PET cases were found to be arrhythmogenic cardiomyopathy. The test

Correspondence to: Marcelo F. Di Carli, MD, Brigham & Women's Hospital, 75 Francis Street, ASB-L1 037C, Boston, MA 02115, Tel: 1 617-732-6291, Fax: 1 617-582-6056, mdicarli@bwh.harvard.edu.

Disclosures: Dr. Padera has served as a consultant for Medtronic. Dr. Mehra is a consultant for Abbott, Medtronic, Janssen (a division of Johnson and Johnson), Mesoblast, Portola, and NupulaseCV. Dr. Desai has received research grants from Novartis. Dr. Kwong has received research grant support from GlaxoSmithKline, Myokardia, and the Society for Cardiovascular Magnetic Resonance. Dr. Ghoshhajra has been a consultant for Siemens Healthcare and Medtronic. Dr. Dorbala is a member of an advisory board for General Electric Health Care. Dr. Di Carli has received consulting fees from Sanofi and General Electric. All other authors have reported that they have no relationships relevant to the contents of this paper to disclose.

characteristics of cardiac MRI are more challenging to comment on using our data as there was only one confirmed case of CS on post-transplant histologic assessment. Of the eight CS highly probable or probable cases by cardiac MRI, three were found to be dilated cardiomyopathy and two were found to be end-stage hypertrophic cardiomyopathy.

Conclusions: FDG PET and cardiac MRI can help facilitate the diagnosis of CS in patients with advanced heart failure with a high degree of sensitivity, but lower specificity.

Keywords

Cardiac sarcoidosis; fluorodeoxyglucose (FDG) positron emission tomography (PET); cardiac magnetic resonance imaging (MRI); cardiac transplantation

Introduction

Sarcoidosis is a multi-system disease characterized by granulomatous inflammation in multiple organs.[1, 2] The etiology of the disease remains unknown, but the theory of an immunologic response to an unknown antigenic trigger causing the disease continues to garner support.[2, 3] Though cardiac involvement manifests clinically in approximately 5% of patients with sarcoidosis, autopsy studies have estimated the prevalence of cardiac involvement to be at least 25%.[4, 5] The three principal clinical manifestations of cardiac sarcoidosis (CS) are conduction disease, ventricular arrhythmias, and heart failure.[2] In patients with clinically present CS, the presence and degree of left ventricular (LV) systolic dysfunction are the most important determinants of prognosis.[6] Progressive heart failure from CS can lead to the need for advanced therapies, such as intravenous inotropes, implantation of a ventricular assist device, and/or cardiac transplantation.

The presence of noncaseating granulomas on endomyocardial biopsy is the current gold standard for the diagnosis of CS.[7, 8] However, the procedure is often not performed because the diagnostic yield is low, even with electroanatomic mapping or image-guidance (20–50%).[2, 7, 9, 10] This has made it historically challenging to confirm the diagnosis in suspected cases of CS with histology. Due to this and other important factors, advanced imaging plays an important role in the management of suspected cases of CS. Fluorodeoxyglucose (FDG) positron emission tomography (PET) is used in the diagnosis of CS, to monitor disease activity, and to guide and assess response to therapy.[7, 11, 12] Cardiac magnetic resonance imaging (MRI) is also used as a diagnostic and prognostic tool in CS, and the two modalities offer complementary value in the assessment of cardiac sarcoidosis.[2, 13] However, there is some controversy about the sensitivity and specificity of advanced imaging findings in suspected cases of CS.

We aimed to correlate findings from FDG PET and cardiac MRI with histologic findings from explanted hearts of patients who underwent cardiac transplantation for advanced heart failure to study the sensitivity and specificity of both imaging modalities for the diagnosis of CS.

Methods

Study Population

The authors declare that all supporting data are available within the article and its online supplementary files. The study population was selected from 213 consecutive patients undergoing cardiac transplantation at Brigham and Women's Hospital (Boston, MA) from April 2008 to July 2018. Eight cases were excluded as they were the second heart transplant for those patients. The pre-transplant clinical diagnoses and post-transplant histologic diagnoses and their frequencies are listed in Supplemental Table 1. All FDG PET and cardiac MRI studies were performed at Brigham and Women's Hospital or Massachusetts General Hospital (Boston, MA). The study was approved by the Partners HealthCare Institutional Review Board and was conducted in accordance with institutional guidelines. Requirement of informed consent was waived.

Advanced imaging studies

Positron emission tomography: The FDG PET protocol has been described in detail elsewhere.[13] Rest myocardial perfusion images were obtained using ^{82}Rubidium (~50 mCi) or ^{13}N-ammonia (~20 mCi) PET/computed tomography (CT) (Discovery RX or DSTE Light Speed 64, GE Healthcare, Milwaukee, WI), or ^{99m}Tc-sestamibi (~20 mCi) single-photon emission computed tomography (SPECT)/CT (Symbia T6, Siemens Healthcare, Hoffman Estates, Chicago, IL). After perfusion imaging, 10–12 mCi of ^{18}F-fluorodeoxyglucose (FDG) was used to perform dedicated cardiac and whole body FDG PET/CT scans.

All patients were instructed to follow a high fat, very low carbohydrate diet (at least two meals) followed by a fast of at least four hours prior to the test to shift normal myocardial metabolism to primary fatty acid utilization and, therefore, suppress the uptake of FDG by normal myocardium.[14, 15]

Image analysis: Rest perfusion images were classified as normal or abnormal. Regional myocardial perfusion was categorized as: normal or mildly, moderately, or severely reduced.[16] FDG images were considered normal when there was no myocardial FDG uptake. In contrast, FDG images were considered abnormal when there was focal, heterogenous, or focal on diffuse myocardial FDG uptake.[11, 14]

Cardiac magnetic resonance imaging: The cardiac MRI protocol has been described in detail elsewhere.[13] All images were acquired on a 3.0-T system (Tim Trio, Siemens, Erlangen, Germany). Cine steady-state free-precession imaging (repetition time, 3.4 ms; echo time, 1.2 ms; in-plane spatial resolution, 1.6–2mm) was used to assess LV function. Late gadolinium enhancement (LGE) imaging was done using inversion recovery gradient recall echo (repetition time, 4.8 ms; echo time, 1.3 ms; inversion time, 200 to 300 ms). LGE imaging was performed with 0.15-mmol/kg dose of gadolinium diethylenetriamine pentaacetic acid (Magnevist, Bayer HealthCare Pharmaceuticals Inc., Wayne, NJ) or gadobenate dimeglumine (Multihance, Bracco Diagnostic, Princeton, NJ). LGE images were obtained in 8 to 14 matching short-axis (8 mm thick with no gap) and 3 long-axis planes.

Image analysis: The presence and pattern of LGE was classified as sub-endocardial, mid-myocardial, and/or sub-epicardial.

Imaging Diagnosis of CS: The likelihood of CS based on FDG PET and/or cardiac MRI data was categorized according to the criteria listed in Table 1.[13] This was done blinded to all clinical and histologic data.

Clinical Data

Review of the electronic health record was used to obtain notable clinical history prior to FDG PET and/or cardiac MRI, the pre-transplant clinical diagnosis, and the post-transplant histologic diagnosis. All pre-imaging and pre-transplant data review was done blinded to imaging and histology results.

Histologic Assessment

The explanted hearts were reviewed by the Cardiovascular Pathology Service at Brigham and Women's Hospital by experienced cardiovascular pathologists according to standard methods.[17] The hearts were reviewed fresh, weighed and fixed in formalin, after which a detailed gross dissection was performed. Representative histologic sections, stained with hematoxylin and eosin (H&E), were taken for light microscopic evaluation; additional special stains were evaluated as necessary.

Statistical Analysis

Baseline patient characteristics were reported as frequencies with percent (%) and means with standard deviations (SD) where appropriate. FDG PET and cardiac MRI studies were categorized as positive or negative using two different cutoffs (highly probable or highly probable/probable). Based on this binomial distribution, sensitivity and specificity, along with exact 95% confidence intervals (CI) using the method of Clopper and Pearson, were calculated for all FDG PET and cardiac MRI studies. Histologic diagnosis of the explanted heart was used as the gold standard test where positive = CS and negative = alternative histologic diagnosis. We compared the differences between mean time (in months) between FDG PET or cardiac MRI and cardiac transplantation and CS probability (unlikely, possible, probable, or highly probable) by FDG PET or cardiac MRI using one-way ANOVA.

Results

The pre-transplant clinical diagnosis and post-transplant histologic diagnosis of the entire patient cohort are described in Supplemental Table 1. Of the 205 patients in our cohort, eighteen (8.8%) underwent FDG PET, 31 (15.1%) underwent cardiac MRI, and seven (3.4%) underwent both during their pre-transplant course. The notable pre-imaging clinical history, pre-transplant clinical diagnosis, and post-transplant histologic diagnosis are listed for all patients who underwent FDG PET and cardiac MRI in Supplemental Tables 2 and 3, respectively. Data for the seven patients who underwent both studies are listed in Supplemental Table 4. We did not find a correlation between CS probability by FDG PET or cardiac MRI and time between imaging study and transplantation (p=0.829 and p=0.359, respectively).

Of the 18 FDG PET studies, the diagnosis of CS was considered highly probable in five, probable in nine, and possible in four cases. None of the studies were classified as CS unlikely (Supplemental Table 2 **and** Table 2). All five cases classified as highly probable for CS had evidence of extracardiac FDG uptake and were confirmed to be CS by post-transplant histologic diagnosis (Supplemental Table 2, Figure 1). Of the nine cases classified as CS probable, only one was confirmed to be CS, three were found to be arrhythmogenic cardiomyopathy (AC) (Figure 2), two were found to be dilated cardiomyopathy (DCM), one was found to be hypertrophic cardiomyopathy (HCM), one was found to be multifocal lymphocytic myocarditis, and one was found to be restrictive cardiomyopathy by post-transplant histologic diagnosis (Supplemental Table 2). Of note, none of these nine cases had evidence of extracardiac FDG uptake. Of the four cases classified as CS possible, two were found to be LMNA-mutation related cardiomyopathy, one was found to be restrictive cardiomyopathy due to lymphocytic myocarditis, and one was found to be dilated cardiomyopathy by post-transplant histologic diagnosis (Supplemental Table 2). None of these four cases had evidence of extracardiac FDG uptake. These results are summarized in Table 2. Additionally, the test characteristics for FDG cardiac PET using post-transplant histologic diagnosis as the gold standard are shown in Table 2. Using a CS highly probable cutoff resulted in a sensitivity of 83.3% (95% CI: 35.9% - 96.6%) and a specificity of 100.0% (95% CI: 73.5% - 100.0%). Using a CS probable cutoff resulted in a sensitivity of 100.0% (95% CI: 54.1% to 100.0%) and a specificity of 33.3% (95% CI: 9.9% - 65.1%). Including the presence of extracardiac FDG uptake as criterion for the probable category would have resulted in a sensitivity of 83.3% (95% CI: 35.9% to 99.6%) and specificity of 100.0% (95% CI 73.5% to 100.0%) using a CS probable cutoff. As all patients in the highly probable category had evidence of extracardiac FDG uptake, this would have resulted in no change in diagnostic accuracy using a CS highly probable cutoff.

Of the 31 cardiac MRI studies, the diagnosis of CS was considered highly probable in four cases, probable in four cases, possible in five cases, and unlikely in 18 cases (Supplemental Table 3 **and** Table 3). One of the four cases classified as CS highly probable was confirmed to be CS by post-transplant histologic diagnosis (Table 3, Figure 3). The other three cases were found to be end-stage HCM, restrictive cardiomyopathy, and DCM by post-transplant histologic diagnosis (Supplemental Table 3). Of the four cases classified as CS probable by cardiac MRI, two were found to be DCM (Figure 4), one was found to be antiphospholipid antibody syndrome (APLAS), and one was found to be end-stage HCM by post-transplant histologic diagnosis (Supplemental Table 3). Of the five cases classified as CS possible by cardiac MRI, four were found to be DCM and one was found to be LMNA-mutation related cardiomyopathy by post-transplant histologic diagnosis (Supplemental Table 3). The details of the 18 CS unlikely by cardiac MRI cases are listed in Supplemental Table 3. All results are summarized in Table 3. Additionally, the test characteristics for cardiac MRI using post-transplant histologic diagnosis as the gold standard are shown in Table 3. As there was only one confirmed case of CS on review of explant histology in the cardiac MRI cohort, the sensitivity 95% confidence intervals are quite large (2.5% - 100%). Therefore, we only report specificity values for cardiac MRI. Using a CS highly probable cutoff resulted in a specificity of 90.0% (95% CI: 73.5% - 97.9%). Using a CS probable cutoff for cardiac MRI resulted in a specificity of 76.7% (95% CI: 57.7% to 90.1%).

Discussion

The poor yield of endomyocardial biopsy in cases of suspected CS has made it historically challenging to assess the sensitivity and specificity of advanced imaging modalities in the diagnosis of CS. Though the characteristics of patients who have undergone cardiac transplantation for CS have previously been studied[18-20], no study to our knowledge has assessed the relationship between the pre-transplant imaging findings in patients with suspected CS and the post-transplant histologic diagnosis of the explanted heart. The use of this histologic assessment as the gold standard for diagnosis is a novel attribute and strength of our study. We demonstrate that FDG PET has high sensitivity using a CS probable cutoff, and a high specificity using a CS highly probable cutoff. The test characteristics of cardiac MRI are more challenging to comment on using our data as there was only one confirmed case of CS on post-transplant histologic assessment. However, we demonstrate a high specificity for cardiac MRI using a CS highly probable cutoff.

It is important to note that all of the CS highly probable by FDG PET cases had abnormal extracardiac uptake on PET, and all were confirmed to be CS on post-transplant histologic assessment. In clinical practice, the diagnosis of CS is usually not in question when a patient's FDG PET reveals multiple areas of focal FDG uptake in the myocardium and extracardiac FDG uptake is present. Our results support this clinical assessment: **FDG PET had a specificity of 100.0% (95% CI: 73.5% - 100.0%) using a highly probable cutoff**.

Using a CS probable cutoff increased the sensitivity of FDG PET to detect CS to 100.0% (95% CI: 54.1% - 100.0%) by correctly identifying one more case of CS without evidence of abnormal extracardiac FDG uptake. However, using this cutoff was associated with a marked reduction in specificity. Indeed, eight of the nine cases classified as probable for CS were found not to be CS on post-transplant histologic assessment. We believe this may be the most impactful finding from our study. As discussed, the sensitivity of FDG PET for the diagnosis of CS is high, but the specificity has room for improvement, particularly in cases without abnormal extracardiac FDG uptake. This is due, at least in part, to the fact that FDG is not a specific imaging tracer for CS and that other conditions associated with myocardial inflammation can confound the diagnosis. Although the specificity of FDG PET could be improved by requiring abnormal extracardiac FDG uptake for a CS probable classification, the sensitivity would drop due to missing isolated CS cases. Our data suggest that one should pause to consider alternate diagnoses (such as AC, LMNA-mutation related cardiomyopathy, and myocarditis (including giant cell myocarditis)) in cases considered probable or highly probable for CS based on FDG PET, especially when abnormal extracardiac FDG uptake is absent.

Of interest, three of the eight cases considered probable for CS by FDG PET were found to be AC on post-transplant histologic review. The fact that CS and AC can mimic each other has been previously reported.[21, 22] A recent exploratory study also showed that some patients with AC can have evidence of myocardial inflammation on FDG PET.[23] However, no study to our knowledge has proposed that clinicians should be suspicious of the diagnosis of AC in a patient with a highly probable or probable diagnosis for CS based on FDG PET result, especially in the absence of abnormal extracardiac FDG uptake. The presence of

inflammatory cells in AC has been previously described,[24] and may be the cause of positive FDG PET results. With the caveat that our cohort is highly selected and small, the results of our study suggest that cardiologists should obtain a detailed family history of at least three generations, as recommended by the recent Heart Failure Society of America guideline[25], and consider genetic testing for AC in patients with a cardiomyopathy and FDG PET results suggestive of isolated CS.

The presented test characteristics of cardiac MRI in the diagnosis of CS in our cohort should be viewed carefully and cautiously as there was only one case of confirmed CS on post-transplant histologic review. However, the alternate diagnoses for the highly probable or probable for CS by cardiac MRI cases are important to review and understand as they may have clinical implications. Of the seven cases that were found not to be CS on post-transplant histologic review, three were found to be DCM, two end-stage HCM, one restrictive cardiomyopathy, and one was found to APLAS by post-transplant histologic diagnosis. It is important to keep in mind that there is overlap in the pattern of LGE among nonischemic cardiomyopathies, and our data are in keeping with this fact. The routine use of myocardial T2 imaging (not available in most of the patients in our cohort) can complement LGE and may help with the diagnosis of inflammatory cardiomyopathies[26]. Consequently, these alternate diagnoses should be kept in mind, particularly DCM and end-stage HCM, when follow up diagnostics are not as supportive of the diagnosis of CS. For example, Subject Number 162 in our study had a cardiac MRI that was CS highly probable, but an FDG PET that was only CS possible. The post-transplant histologic diagnosis for this case was DCM (Figure 4). Additionally, obtaining a detailed family history and/or careful consideration of genetic testing may uncover a diagnosis HCM.

As mentioned, our study has important limitations. The study represents a single center experience that included a relatively small cohort of subjects who underwent FDG PET imaging and/or cardiac MRI for suspected CS before transplantation. Selection bias may be present in our study as our institution is a referral center for both CS and genetic cardiomyopathies. Some patients also had advanced cardiac imaging at outside centers and these were not included in our analysis. The results, however, were incorporated into the patients' histories. Our patients represent a highly-selected cohort in which all patients developed progressive end-stage heart failure requiring cardiac transplantation. Additionally, the use of FDG PET to detect inflammation may be limited in cases of severe heart failure due to preferential glucose utilization by the myocardium regardless of patient preparation/dietary adherence.[27] Nevertheless, these results may have clinical implications for the diagnostic algorithm for patients with suspected CS and the management of patients with abnormal FDG PET results. They also may invite more research into perfusion and metabolic imaging of patients with suspected or confirmed AC.

Conclusions

FDG PET and cardiac MRI help to facilitate the diagnosis of CS in patients with advanced heart failure with a high degree of sensitivity, but lower specificity. More work is needed to investigate further the diagnosis of isolated CS by FDG PET, better define the potential role of genetic testing in potential isolated CS cases by FDG PET and highly probable or

probable CS cases by cardiac MRI with incongruent follow up diagnostics, and the potential role of perfusion and metabolic imaging of patients with suspected or confirmed AC.

Supplementary Material

Refer to Web version on PubMed Central for supplementary material.

Acknowledgments

Sources of Funding: Dr. Divakaran and Dr. Zhou are supported by grant number T32 HL094301 from the National Heart, Lung, and Blood Institute. Dr. Stewart is supported by the Kenneth L. Baughman Master Clinician Scholar Program in Cardiovascular Medicine at Brigham and Women's Hospital. Dr. Kwong is supported by grant number 1UH2 TR000901 from the National Institutes of Health. Dr. Taqueti is supported by grant number K23 HL135438 from the National Heart, Lung, and Blood Institute. Dr. Dorbala is supported by grant number R01 HL130563 from the National Heart, Lung, and Blood Institute. Dr. Di Carli is supported by grant number R01 HL132021 from the National Heart, Lung, and Blood Institute.

References

1. Iannuzzi MC, Fontana JR. Sarcoidosis: clinical presentation, immunopathogenesis, and therapeutics. JAMA. 2011;305:391–399. [PubMed: 21266686]
2. Birnie DH, Nery PB, Ha AC, Beanlands RS. Cardiac Sarcoidosis. J Am Coll Cardiol. 2016;68:411–421. [PubMed: 27443438]
3. McGrath DS, Goh N, Foley PJ, du Bois RM. Sarcoidosis: genes and microbes--soil or seed? Sarcoidosis Vasc Diffuse Lung Dis. 2001;18:149–164. [PubMed: 11436535]
4. Silverman KJ, Hutchins GM, Bulkley BH. Cardiac sarcoid: a clinicopathologic study of 84 unselected patients with systemic sarcoidosis. Circulation. 1978;58:1204–1211. [PubMed: 709777]
5. Iwai K, Tachibana T, Takemura T, Matsui Y, Kitaichi M, Kawabata Y. Pathological studies on sarcoidosis autopsy. I. Epidemiological features of 320 cases in Japan. Acta Pathol Jpn. 1993;43:372–376. [PubMed: 8372682]
6. Yazaki Y, Isobe M, Hiroe M, Morimoto S, Hiramitsu S, Nakano T, Izumi T, Sekiguchi M, Group CJHS. Prognostic determinants of long-term survival in Japanese patients with cardiac sarcoidosis treated with prednisone. Am J Cardiol. 2001;88:1006–1010. [PubMed: 11703997]
7. Birnie DH, Sauer WH, Bogun F, Cooper JM, Culver DA, Duvernoy CS, Judson MA, Kron J, Mehta D, Cosedis Nielsen J, Patel AR, Ohe T, Raatikainen P, Soejima K. HRS expert consensus statement on the diagnosis and management of arrhythmias associated with cardiac sarcoidosis. Heart Rhythm. 2014;11:1305–1323. [PubMed: 24819193]
8. Judson MA, Costabel U, Drent M, Wells A, Maier L, Koth L, Shigemitsu H, Culver DA, Gelfand J, Valeyre D, Sweiss N, Crouser E, Morgenthau AS, Lower EE, Azuma A, Ishihara M, Morimoto S, Tetsuo Yamaguchi T, Shijubo N, Grutters JC, Rosenbach M, Li HP, Rottoli P, Inoue Y, Prasse A, Baughman RP, Organ Assessment Instrument Investigators TW. The WASOG Sarcoidosis Organ Assessment Instrument: An update of a previous clinical tool. Sarcoidosis Vasc Diffuse Lung Dis. 2014;31:19–27. [PubMed: 24751450]
9. Nery PB, Keren A, Healey J, Leug E, Beanlands RS, Birnie DH. Isolated cardiac sarcoidosis: establishing the diagnosis with electroanatomic mapping-guided endomyocardial biopsy. Can J Cardiol. 2013;29:1015.e1–3.
10. Liang JJ, Hebl VB, DeSimone CV, Madhavan M, Nanda S, Kapa S, Maleszewski JJ, Edwards WD, Reeder G, Cooper LT, Asirvatham SJ. Electrogram guidance: a method to increase the precision and diagnostic yield of endomyocardial biopsy for suspected cardiac sarcoidosis and myocarditis. JACC Heart Fail. 2014;2:466–473. [PubMed: 25194292]
11. Ishimaru S, Tsujino I, Takei T, Tsukamoto E, Sakaue S, Kamigaki M, Ito N, Ohira H, Ikeda D, Tamaki N, Nishimura M. Focal uptake on 18F-fluoro-2-deoxyglucose positron emission tomography images indicates cardiac involvement of sarcoidosis. Eur Heart J. 2005;26:1538–1543. [PubMed: 15809286]

12. Chareonthaitawee P, Beanlands RS, Chen W, Dorbala S, Miller EJ, Murthy VL, Birnie DH, Chen ES, Cooper LT, Tung RH, White ES, Borges-Neto S, Di Carli MF, Gropler RJ, Ruddy TD, Schindler TH, Blankstein R. Joint SNMMI-ASNC expert consensus document on the role of. J Nucl Cardiol. 2017;24:1741–1758. [PubMed: 28770463]
13. Vita T, Okada DR, Veillet-Chowdhury M, Bravo PE, Mullins E, Hulten E, Agrawal M, Madan R, Taqueti VR, Steigner M, Skali H, Kwong RY, Stewart GC, Dorbala S, Di Carli MF, Blankstein R. Complementary Value of Cardiac Magnetic Resonance Imaging and Positron Emission Tomography/Computed Tomography in the Assessment of Cardiac Sarcoidosis. Circ Cardiovasc Imaging. 2018;11:e007030. [PubMed: 29335272]
14. Blankstein R, Osborne M, Naya M, Waller A, Kim CK, Murthy VL, Kazemian P, Kwong RY, Tokuda M, Skali H, Padera R, Hainer J, Stevenson WG, Dorbala S, Di Carli MF. Cardiac positron emission tomography enhances prognostic assessments of patients with suspected cardiac sarcoidosis. J Am Coll Cardiol. 2014;63:329–336. [PubMed: 24140661]
15. Osborne MT, Hulten EA, Murthy VL, Skali H, Taqueti VR, Dorbala S, DiCarli MF, Blankstein R. Patient preparation for cardiac fluorine-18 fluorodeoxyglucose positron emission tomography imaging of inflammation. J Nucl Cardiol. 2017;24:86–99. [PubMed: 27277502]
16. Tilkemeier PL, Wackers FJ, Cardiology QACotASoN. Myocardial perfusion planar imaging. J Nucl Cardiol. 2006;13:e91–6. [PubMed: 17174799]
17. Stone JR, Basso C, Baandrup UT, Bruneval P, Butany J, Gallagher PJ, Halushka MK, Miller DV, Padera RF, Radio SJ, Sheppard MN, Suvarna K, Tan CD, Thiene G, van der Wal AC, Veinot JP. Recommendations for processing cardiovascular surgical pathology specimens: a consensus statement from the Standards and Definitions Committee of the Society for Cardiovascular Pathology and the Association for European Cardiovascular Pathology. Cardiovasc Pathol. 2012;21:2–16. [PubMed: 21353600]
18. Roberts WC, Chung MS, Ko JM, Capehart JE, Hall SA. Morphologic features of cardiac sarcoidosis in native hearts of patients having cardiac transplantation. Am J Cardiol. 2014;113:706–712. [PubMed: 24393258]
19. Akashi H, Kato TS, Takayama H, Naka Y, Farr M, Mancini D, Schulze PC. Outcome of patients with cardiac sarcoidosis undergoing cardiac transplantation--single-center retrospective analysis. J Cardiol. 2012;60:407–410. [PubMed: 22890069]
20. Zaidi AR, Zaidi A, Vaitkus PT. Outcome of heart transplantation in patients with sarcoid cardiomyopathy. J Heart Lung Transplant. 2007;26:714–717. [PubMed: 17613402]
21. Vasaiwala SC, Finn C, Delpriore J, Leya F, Gagermeier J, Akar JG, Santucci P, Dajani K, Bova D, Picken MM, Basso C, Marcus F, Wilber DJ. Prospective study of cardiac sarcoid mimicking arrhythmogenic right ventricular dysplasia. J Cardiovasc Electrophysiol. 2009;20:473–476. [PubMed: 19017339]
22. Corrado D, Thiene G. Cardiac sarcoidosis mimicking arrhythmogenic right ventricular cardiomyopathy/dysplasia: the renaissance of endomyocardial biopsy? J Cardiovasc Electrophysiol. 2009;20:477–479. [PubMed: 19207751]
23. Protonotarios A, Wicks E, Ashworth M, Stephenson E, Guttmann O, Savvatis K, Sekhri N, Mohiddin SA, Syrris P, Menezes L, Elliott P. Prevalence of 18F-fluorodeoxyglucose positron emission tomography abnormalities in patients with arrhythmogenic right ventricular cardiomyopathy. Int J Cardiol. 2019; 284:99–104. [PubMed: 30409737]
24. Asimaki A, Saffitz JE. The role of endomyocardial biopsy in ARVC: looking beyond histology in search of new diagnostic markers. J Cardiovasc Electrophysiol. 2011;22:111–117. [PubMed: 21235662]
25. Hershberger RE, Givertz MM, Ho CY, Judge DP, Kantor PF, McBride KL, Morales A, Taylor MRG, Vatta M, Ware SM. Genetic Evaluation of Cardiomyopathy-A Heart Failure Society of America Practice Guideline. J Card Fail. 2018;24:281–302. [PubMed: 29567486]
26. Crouser ED, Ono C, Tran T, He X, Raman SV. Improved detection of cardiac sarcoidosis using magnetic resonance with myocardial T2 mapping. Am J Respir Crit Care Med. 2014;189:109–112. [PubMed: 24381994]
27. Dávila-Román VG, Vedala G, Herrero P, de las Fuentes L, Rogers JG, Kelly DP, Gropler RJ. Altered myocardial fatty acid and glucose metabolism in idiopathic dilated cardiomyopathy. J Am Coll Cardiol. 2002;40:271–277. [PubMed: 12106931]

Clinical Perspective

The diagnostic yield of CS by endomyocardial biopsy is limited. FDG PET and cardiac MRI may facilitate noninvasive diagnosis, but the accuracy of this approach is not well defined. We aimed to correlate findings from FDG PET and cardiac MRI with histologic findings from explanted hearts of patients who underwent cardiac transplantation. We analyzed the explanted heart histology for all patients who underwent cardiac transplant at our center from April 2008 to July 2018 and had pre-transplant FDG PET (n=18) or cardiac MRI (n=31). The likelihood of CS based on FDG PET or cardiac MRI was categorized in a blinded fashion using a previously published method. Of the eight CS probable by FDG PET cases that were not found to be CS, three were found to be arrhythmogenic cardiomyopathy. Of the seven CS highly probable or probable cases by cardiac MRI that were not found to be CS, three were found to be dilated cardiomyopathy and two were found to be end-stage hypertrophic cardiomyopathy. We found that FDG PET and cardiac MRI can help facilitate the diagnosis of CS in patients with advanced heart failure with a high degree of sensitivity, but lower specificity.

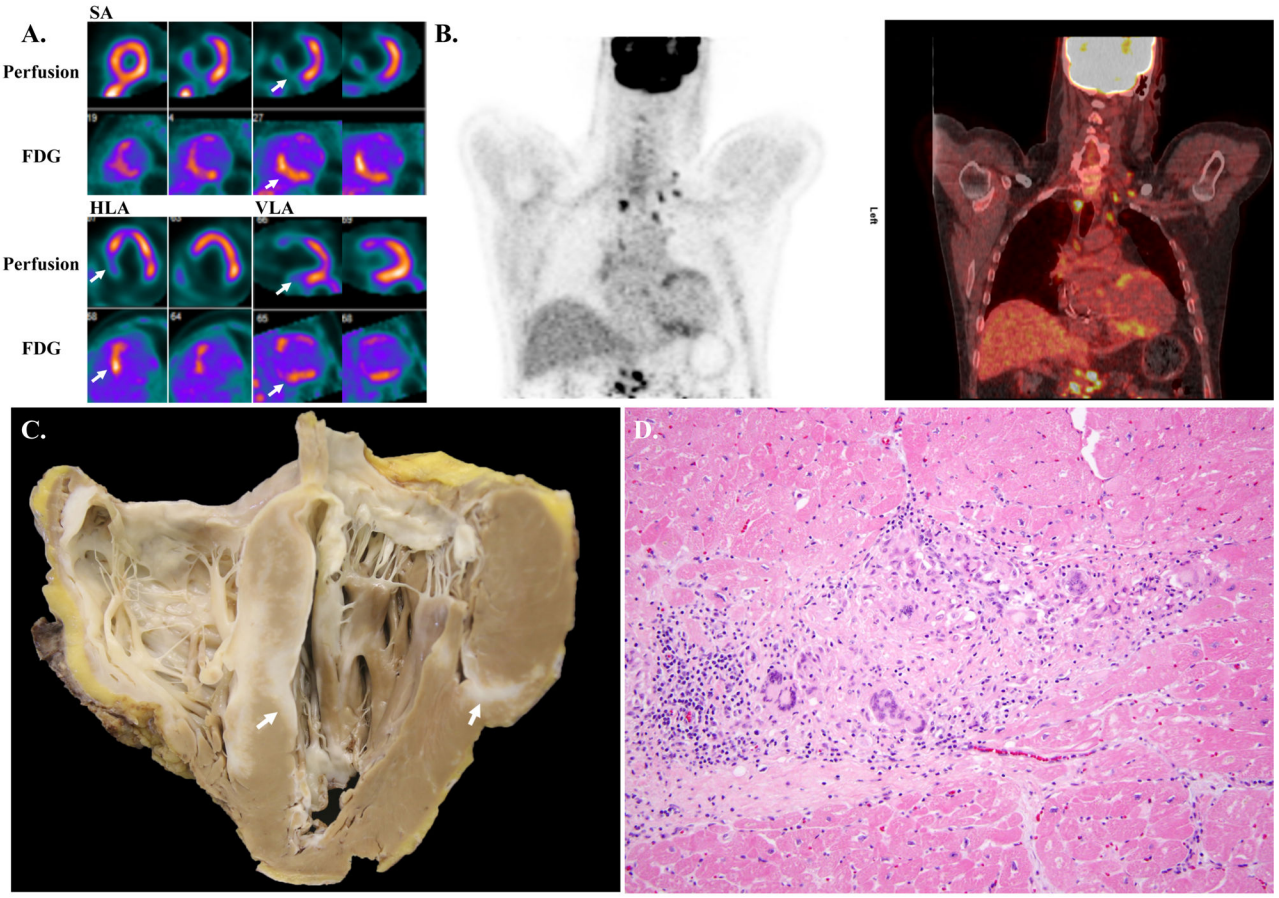

Figure 1. Example fluorodeoxyglucose positron emission tomography images and histology images of a case of cardiac sarcoidosis.

A. Short axis (SA), horizontal long axis (HLA), and vertical long axis (VLA) ^{99m}Tc-sestamibi myocardial perfusion SPECT and FDG PET imaging showing perfusion defects with FDG uptake in the mid and basal anteroseptal and inferoseptal segments (arrows). This study was deemed CS highly probable given the mismatched defects.

B. Coronal PET (left) and PET/CT whole body FDG imaging showing anteroseptal and inferoseptal myocardial uptake, as well as multiple FDG-avid bilateral mediastinal, bilateral hilar, and upper abdominal lymph nodes.

C. Gross photograph of four-chamber view of the explanted heart showing diffuse involvement of the myocardium by sarcoid (arrows). The right ventricle is extensively involved, as is the interventricular septum, with more patchy involvement of the left ventricle.

D. Photomicrograph of H&E stained section showing myocardium with a non-necrotizing granuloma containing abundant giant cells. There is fibrosis and a lymphocytic infiltrate at the periphery of the granuloma. (200X original magnification)

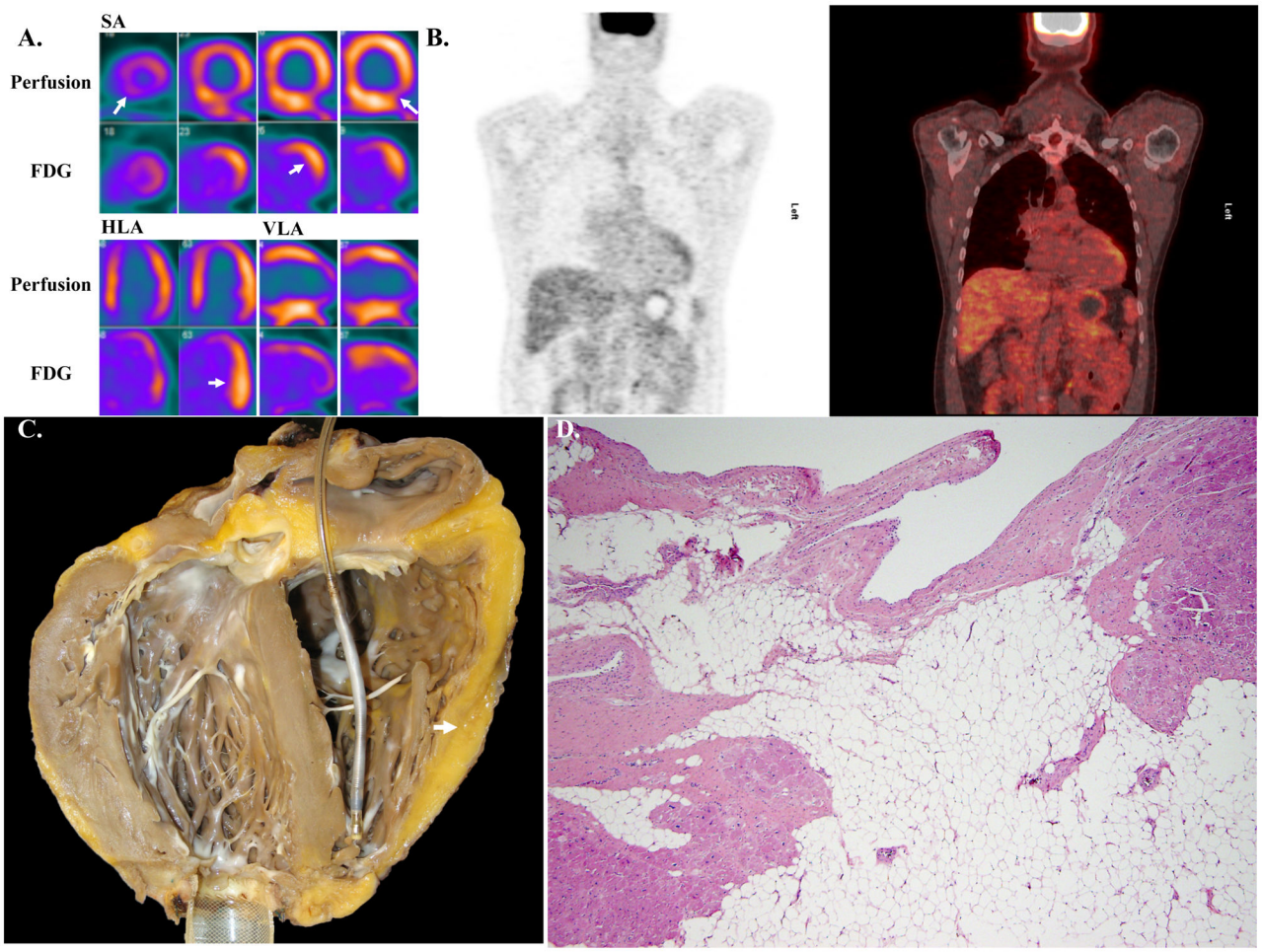

Figure 2. Example fluorodeoxyglucose positron emission tomography images and histology images of a case of arrhythmogenic cardiomyopathy.

A. Short axis (SA), horizontal long axis (HLA), and vertical long axis (VLA) ^{99m}Tc-sestamibi myocardial perfusion SPECT and FDG PET imaging showing a medium-sized perfusion defect in the apical anterior, septal, and inferior walls, as well as the left ventricular apex. There is also a small-sized perfusion defect in the basal inferolateral wall (arrows). There is FDG uptake in the apical lateral wall and the mid and basal anterolateral walls (arrows). While this pattern of FDG uptake is generally considered a normal variant, its association with perfusion defects in the absence of obstructive CAD was deemed abnormal and categorized as CS probable.

B. Coronal PET (left) and PET/CT whole body FDG imaging showing anterolateral wall myocardial uptake, and the absence of abnormal extracardiac FDG uptake.

C. Gross photograph of four chamber view of the explanted heart showing fatty replacement of the right ventricular free wall characteristic of AC (arrow). An automatic implantable cardioverter-defibrillator lead is seen in the right heart along with evidence of an apically placed left ventricular assist device.

D. Photomicrograph of H&E stained section demonstrating transmural fibrofatty infiltration of the right ventricular free wall without other significant pathology. Occasional islands of viable myocardium remain. (40X original magnification)

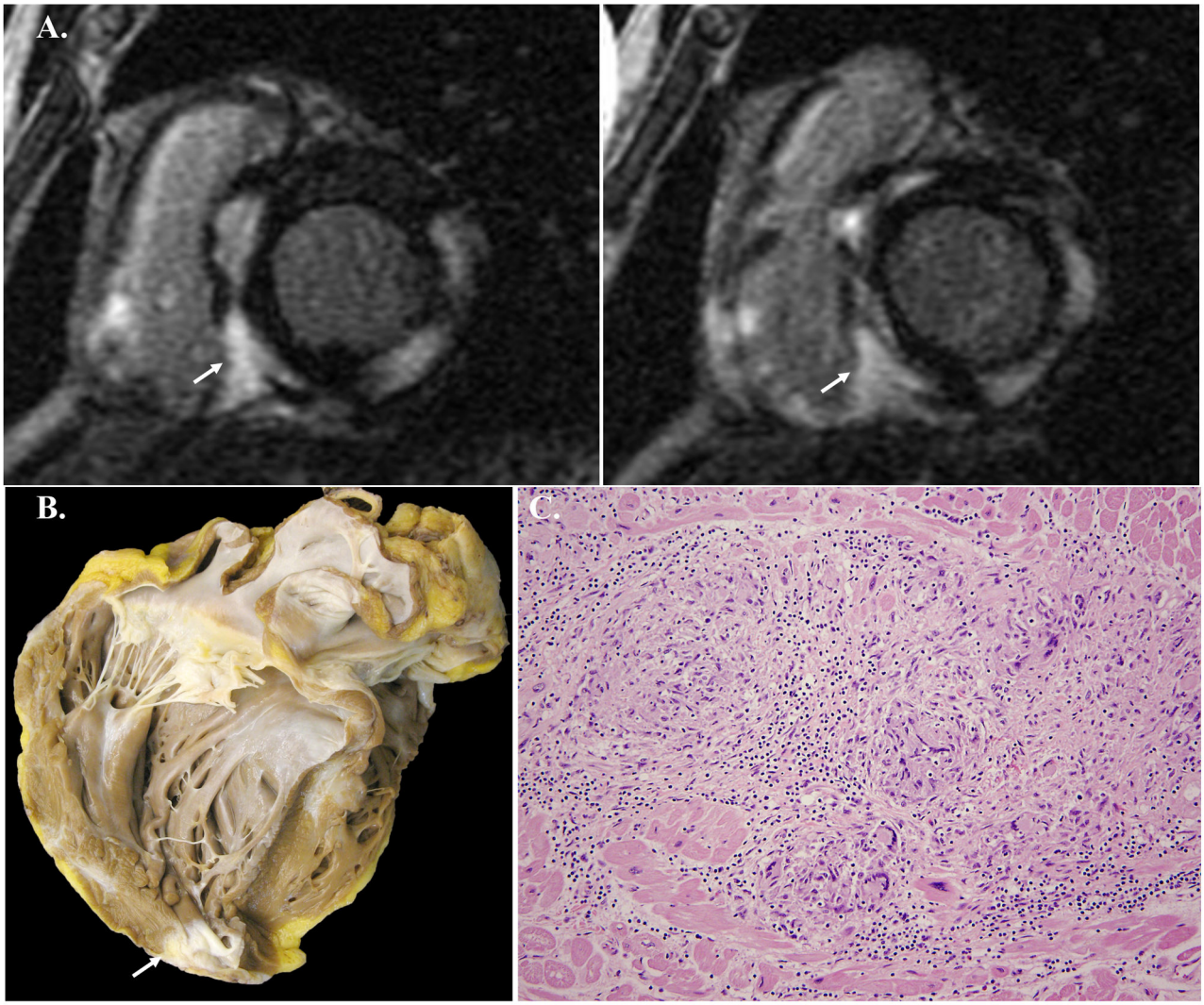

Figure 3. Example cardiac magnetic resonance imaging images and histology images of a case of cardiac sarcoidosis.

A. Short axis cardiac MRI images showing numerous large, focal areas of prominent LGE in the lateral, inferolateral, inferoseptal, and anteroseptal segments of the left ventricle as well as LGE of the right ventricular wall. Direct and contiguous extension of LGE across the interventricular septum into the right ventricle is seen in both images (arrows). This study was deemed CS highly probable given the pattern and location of the LGE.

B. Gross photograph of four chamber view of the explanted heart showing patchy fibrosis of the left ventricular free wall, apex and basal interventricular septum characteristic of myocardial involvement by sarcoid (arrow).

C. Photomicrograph of H&E stained section showing myocardium with a non-necrotizing granuloma containing abundant giant cells. There is a lymphocytic infiltrate at the periphery of the granuloma. (200X original magnification)

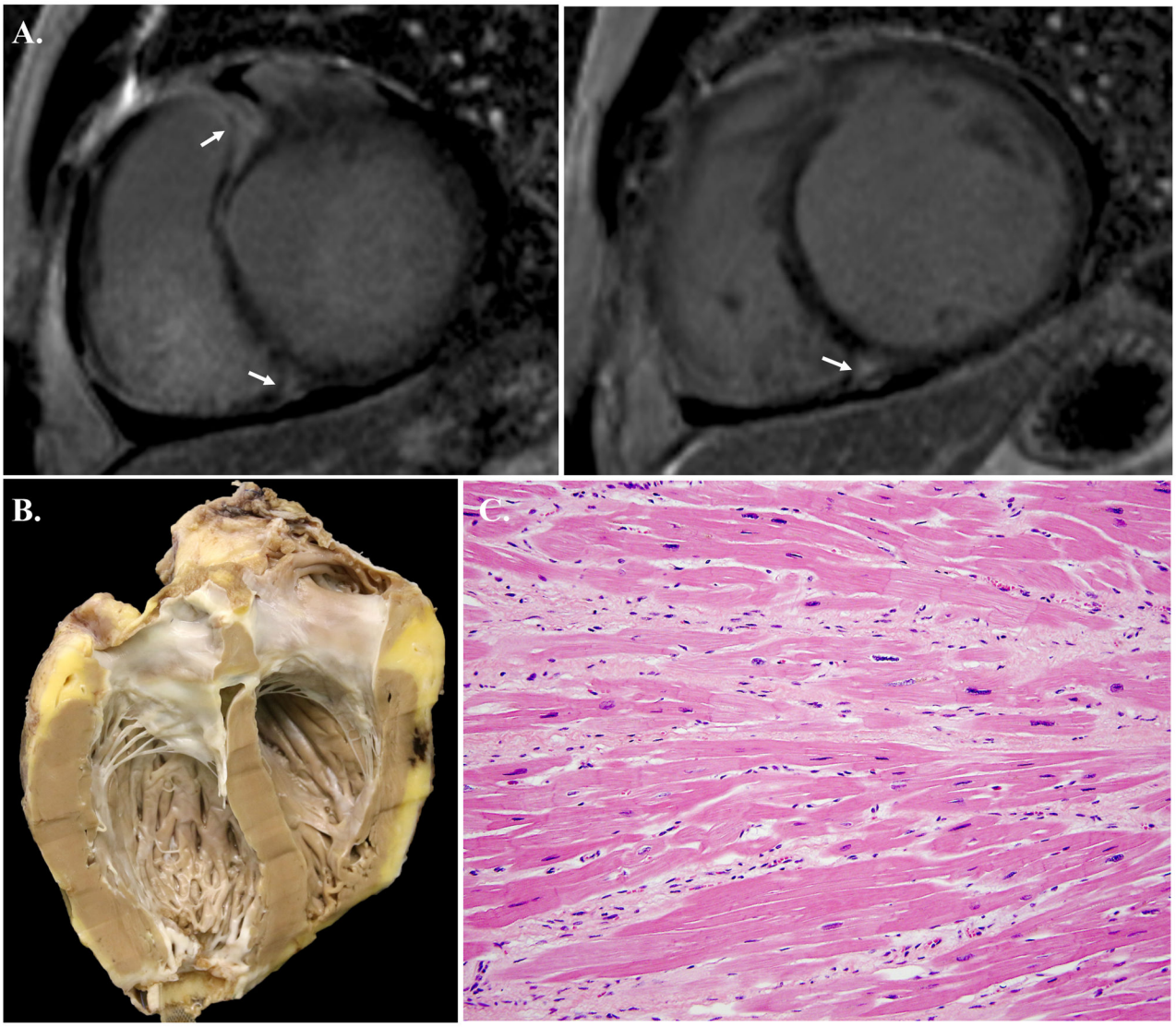

Figure 4. Example cardiac magnetic resonance imaging images and histology images of a case of dilated cardiomyopathy.

A. Short axis cardiac MRI images showing direct and contiguous extension of LGE across the interventricular septum into the right ventricle and focal LGE of basal right ventricular insertions points (arrows). This study was deemed CS highly probable given the pattern and location of the LGE.

B. Gross photograph of four chamber view of the explanted heart showing biventricular dilation and hypertrophy characteristic of DCM. There is evidence of an apically placed left ventricular assist device.

C. Photomicrograph of H&E stained section demonstrating myocyte hypertrophy and interstitial fibrosis without inflammation or other significant pathology. (200X original magnification)

Table 1.

Definitions of criteria used to categorize cardiac sarcoidosis likelihood based on fluorodeoxyglucose positron emission tomography and cardiac magnetic resonance imaging findings.

Likelihood Probability	FDG PET Likelihood	Cardiac MRI Likelihood
CS Unlikely (<10%)	-No perfusion defects and no FDG uptake	-No LGE -LGE present but clear alternative diagnosis (e.g. arrhythmogenic cardiomyopathy, coronary artery disease)
CS Possible (10-50%)	-Single perfusion defect without associated FDG uptake -No perfusion defects, but non-specific FDG uptake *	-One focal area of LGE but alternative diagnosis more likely (e.g. pulmonary hypertension)
CS Probable (50-90%)	-Multiple, non-contiguous perfusion defects without associated FDG uptake -Single perfusion defect with associated focal or focal on diffuse FDG uptake -No perfusion defects, but focal or focal on diffuse FDG uptake	-Multifocal LGE in a pattern that is likely consistent with CS, but cannot rule out other diagnosis (e.g. myocarditis)
CS Highly Probable (>90%)	-Multiple, non-contiguous perfusion defects with associated FDG uptake -Multiple areas of focal FDG uptake and extracardiac FDG uptake present	-Multifocal LGE in a pattern strongly consistent† with CS with no alternative diagnosis

* Non-specific FDG uptake includes the following: (1) diffuse FDG uptake of the left ventricular myocardium and (2) focal FDG uptake with signal intensity that is only minimally increased when compared to background/blood pool uptake. †Features on cardiac MRI strongly consistent with CS: intense signal of LGE and/or prominent involvement of insertion points with direct and contiguous extension across the septum into the right ventricle. CS, cardiac sarcoidosis. FDG, fluorodeoxyglucose. LGE, late gadolinium enhancement. MRI, magnetic resonance imaging. PET, positron emission tomography. Adapted from Vita T et al. Circ Cardiovasc Imaging. 2018 Jan;11(1):e007030.[13]

Table 2.

Test characteristics for fluorodeoxyglucose positron emission tomography.

Post-transplant histologic diagnosis (CS or alternate diagnosis) stratified by FDG PET CS probability and test characteristics for FDG PET for the diagnosis of CS using two different cutoffs and post-transplant histologic diagnosis as the gold standard. 95% CI, exact (Clopper-Pearson) 95% confidence intervals. CS, cardiac sarcoidosis. FDG, fluorodeoxyglucose. PET, positron emission tomography.

FDG PET CS Likelihood Probability	CS	Alternate Histologic Diagnosis
Unlikely	0	0
Possible	0	4
Probable	1	8
Highly Probable	5	0
FDG PET CS Highly Probable	5	0
FDG PET CS Probable, Possible, or Unlikely	1	12
FDG PET CS Highly Probable or Probable	6	8
FDG PET CS Possible or Unlikely	0	4
	Sensitivity (95% CI)	**Specificity (95% CI)**
Highly Probable Cutoff	83.3% (35.9% - 99.6%)	100.0% (73.5% - 100.0%)
	Sensitivity (95% CI)	**Specificity (95% CI)**
Probable Cutoff	100.0% (54.1% - 100.0%)	33.3% (9.9% - 65.1%)

Table 3.
Test characteristics for cardiac magnetic resonance imaging.

Post-transplant histologic diagnosis (CS or alternate diagnosis) stratified by cardiac MRI CS probability and specificity for cardiac MRI for the diagnosis of CS using two different cutoffs and post-transplant histologic diagnosis as the gold standard. 95% CI, exact (Clopper-Pearson) 95% confidence intervals. CS, cardiac sarcoidosis. MRI, magnetic resonance imaging.

Cardiac MRI CS Likelihood Probability	CS	Alternate Histologic Diagnosis
Unlikely	0	18
Possible	0	5
Probable	0	4
Highly Probable	1	3
Cardiac MRI CS Highly Probable	1	3
Cardiac MRI CS Probable, Possible, or Unlikely	0	27
Cardiac MRI CS Highly Probable or Probable	1	7
Cardiac MRI CS Possible or Unlikely	0	23
		Specificity (95% CI)
Highly Probable Cutoff		90.0% (73.5% to 97.9%)
		Specificity (95% CI)
Probable Cutoff		76.7% (57.7% to 90.1%)